

The Project for Intercomparison of Land-surface Parameterization Schemes (PILPS) phase 2(c) Red-Arkansas River basin experiment:

2. Spatial and temporal analysis of energy fluxes

Xu Liang ^{a,*}, Eric F. Wood ^a, Dennis P. Lettenmaier ^b, Dag Lohmann ^a, Aaron Boone ^{c,1}, Sam Chang ^d, Fei Chen ^{e,2}, Yongjiu Dai ^f, Carl Desborough ^g, Robert E. Dickinson ^h, Qingyun Duan ⁱ, Michael Ek ^j, Yeugeniy M. Gusev ^k, Florence Habets ^l, Parviz Irannejad ^m, Randy Koster ⁿ, Kenneth E. Mitchell ^e, Olga N. Nasonova ^k, Joel Noilhan ^l, John Schaake ⁱ, Adam Schlosser ^o, Yaping Shao ^m, Andrey B. Shmakin ^p, Diana Verseghy ^q, Kirsten Warrach ^r, Peter Wetzel ^c, Yongkang Xue ^{s,3}, Zong-Liang Yang ^h, Qing-cun Zeng ^f

^a Department of Civil Engineering and Operations Research, Princeton University, Princeton, NJ, USA

^b Department of Civil Engineering, University of Washington, Seattle, WA, USA

^c Mesoscale Dynamics and Precipitation Branch, NASA / GSFC, Greenbelt, MD, USA

^d Air Force Research Laboratory, Hanscom AFB, Hanscom, MA, USA

^e Environmental Modeling Center (NOAA / NCEP), Camp Springs, MD, USA

^f Institute of Atmospheric Physics, Chinese Academy of Sciences, Beijing, China

^g Climatic Impacts Center, Macquarie University, Sydney, Australia

^h Institute of Atmospheric Physics, University of Arizona, Tucson, AZ, USA

ⁱ Office of Hydrology, NOAA / NWS, Silver Spring, MD, USA

^j Oregon State University, Corvallis, OR, USA

^k Institute of Water Problems, Moscow, Russian Federation

^l Météo-France / CNRM, Toulouse, France

^m Centre for Advanced Numerical Computation in Engineering and Science, The University of N.S.W., New South Wales 2052, Australia

ⁿ Hydrological Sciences Branch, NASA / GSFC, Greenbelt, MD, USA

^o NOAA / GFDL, Princeton, NJ, USA

^p Institute of Geography, Moscow, Russian Federation

^q Climate Research Branch, Atmospheric Environment Service, Toronto, Ontario, Canada

* Corresponding author.

¹ Currently at JCET UMBC/NASA, Climate and Radiation Branch, Code 913, NASA Goddard Space Flight Center, Greenbelt, MD 20771, USA.

² Currently at NCAR, Boulder, CO, USA.

³ Currently at Dept. of Geography, Univ. of Maryland, College Park, MD 20742, USA.

[†] GKSS Research Center, Geesthacht, Germany[§] Center for Ocean-Land-Atmosphere Studies, Calverton, MD, USA

Received 10 September 1997; accepted 9 February 1998

Abstract

The energy components of sixteen Soil-Vegetation Atmospheric Transfer (SVAT) schemes were analyzed and intercompared using 10 years of surface meteorological and radiative forcing data from the Red-Arkansas River basin in the Southern Great Plains of the United States. Comparisons of simulated surface energy fluxes among models showed that the net radiation and surface temperature generally had the best agreement among the schemes. On an average (annual and monthly) basis, the estimated latent heat fluxes agreed (to within approximate estimation errors) with the latent heat fluxes derived from a radiosonde-based atmospheric budget method for slightly more than half of the schemes. The sensible heat fluxes had larger differences among the schemes than did the latent heat fluxes, and the model-simulated ground heat fluxes had large variations among the schemes. The spatial patterns of the model-computed net radiation and surface temperature were generally similar among the schemes, and appear reasonable and consistent with observations of related variables, such as surface air temperature. The spatial mean patterns of latent and sensible heat fluxes were less similar than for net radiation, and the spatial patterns of the ground heat flux vary greatly among the 16 schemes. Generally, there is less similarity among the models in the temporal (interannual) variability of surface fluxes and temperature than there is in the mean fields, even for schemes with similar mean fields. © 1998 Elsevier Science B.V. All rights reserved.

Keywords: PILPS; energy balance; land-surface models; Red-Arkansas River basin

1. Introduction

This paper is Part 2 of a 3-part series summarizing results of Phase 2(c) of the Project for Intercomparison of Land-surface Parameterization Schemes (PILPS). The focus of Part 2 is the evaluation of the energy balances simulated by the 16 models that participated in the PILPS Phase 2(c) experiment. The goal of PILPS is to improve the parameterization of the land surface schemes (LSS) used in climate and weather prediction models. Details of the project are described by Henderson-Sellers et al. (1993) and Henderson-Sellers et al. (1995).

PILPS has facilitated a series of intercomparison experiments. Phase 1 focused on point evaluations using LSS model forcings from NCAR's CCM1-Oz general circulation model for two grid points representative of a tropical forest and a northern hemisphere, mid-latitude grassland (Pitman et al., 1993). Phase 2 progressed to LSS evaluations using field data. In Phase 2(a), observations of latent and sensible heat fluxes from a site at Cabauw, the Netherlands, were compared to model simulations for 23 participating land surface schemes. On an annual

basis, the net radiation range for PILPS Phase 2(a) was found to be about 10 W m^{-2} , and associated ranges in sensible and latent heat fluxes of 30 W m^{-2} and 25 W m^{-2} , respectively (Chen et al., 1997). In Phase 2(b), simulated energy fluxes from 14 schemes were compared with observations from the HAPEX-MOBILHY Caumont site for a 35-day intensive observation period (Shao et al., 1994).

In Phase 2(c), the design of which is described in detail in Part 1 of this series, along with the participating models, (Wood et al., this issue), off-line simulations from 16 land surface schemes were compared to observations of streamflow and basin-scale evapotranspiration in the $566,251 \text{ km}^2$ Red-Arkansas River basin located in the Southern Great Plains region of the USA. Part 3 of this series (Lohmann et al., this issue) evaluates performance of the models in terms of their simulations of surface water fluxes (including streamflow and evapotranspiration).

The PILPS Phase 2(c) experimental design was, briefly, as follows. Participants were provided with surface atmospheric forcings at a 1° scale for 61 grid cells that constitute the Red-Arkansas River basin. They were also provided with forcings for six small

catchments (drainage areas ranging from approximately 100 to 1000 km²), and for three of these ('calibration catchments') they were also provided with the coincident streamflow observations. In the Phase 2(c) experiment, three groups of runs were performed. The first of these is the calibration/validation runs using data from the six small catchments described above. The results from these runs are described in Part 1 (Wood et al., this issue). The second set is a 10-year base-run for the entire Red-Arkansas basin at the 1° scale. A series of sensitivity experiments constituted the third set of runs. Participants were not provided streamflow observations for the validation catchments, the river flows for the major tributaries of the Red-Arkansas, and the basin-wide atmospheric budget derived evapotranspi-

ration, all of which were used for model evaluations and intercomparisons.

Preliminary analyzes and intercomparisons from the PILPS Phase 2(c) runs were presented at a workshop held at Princeton University October 28–31, 1996. As reported by Wood et al. (this issue), some schemes resubmitted results after the workshop due to model errors and other problems with their initial runs. The analyzes reported here are based on the final submittal of each scheme. Seven schemes (ALISIS, BATS, CLASS, MOSAIC, NCEP, PLACE and SEWAB) resubmitted runs after the workshop while the remaining nine (BASE, BUCK, CAPS, IAP94, ISBA, SPONSOR, SSiB, SWAP and VIC-3L) schemes did not. The reasons for the resubmissions are described by Wood et al. (this issue).

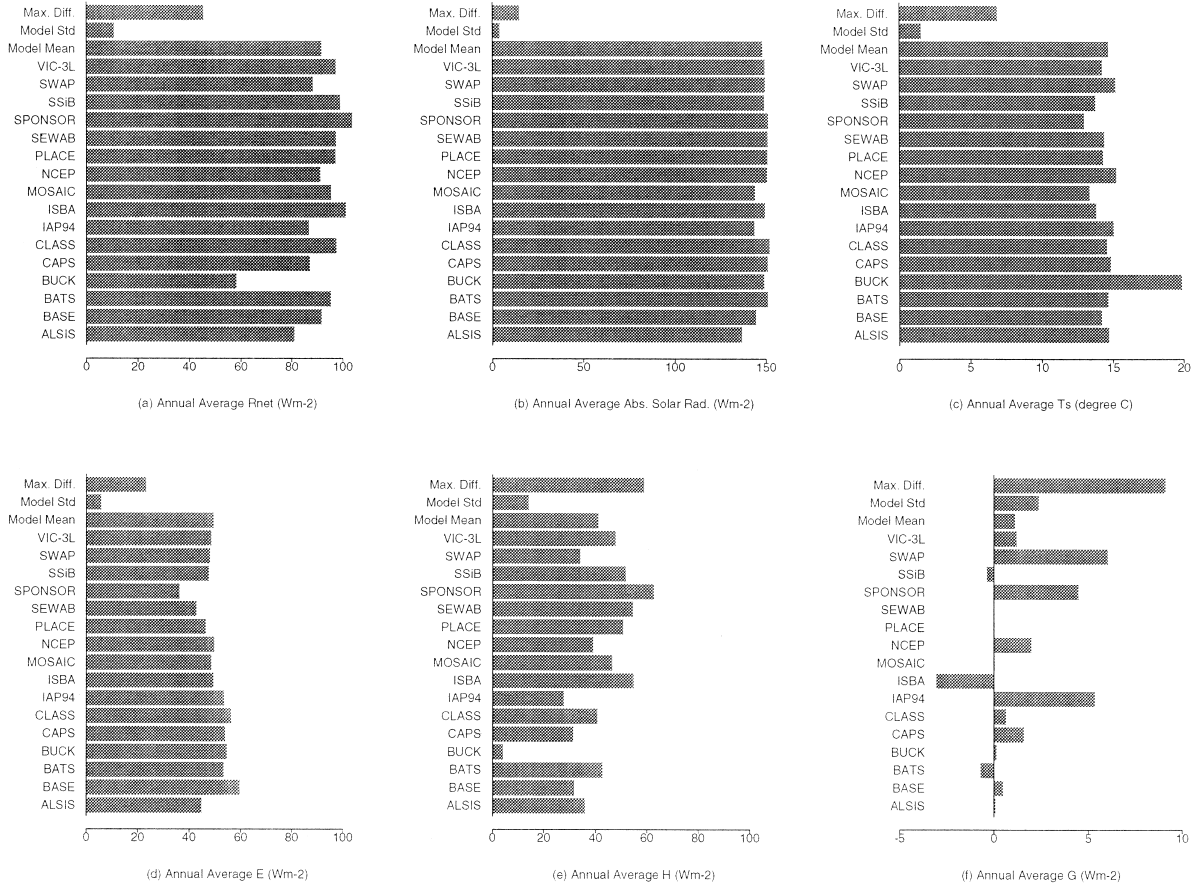


Fig. 1. Annual average model-simulated net radiation, absorbed solar radiation, surface temperature, latent, sensible, and ground heat flux over the Red-Arkansas River basin (1980–1986).

In Part 2 (this paper), the simulated surface energy fluxes from the base-runs are compared among the land surface schemes at the annual, monthly, and diurnal time step for spatial scales ranging from a single 1° grid box to the entire Red-Arkansas basin. Depending on the schemes, the time step for the simulations ranged from 20 min to 3 h (see Table 1, Wood et al., this issue). The model-derived evapotranspiration was aggregated to monthly, basin-averaged values and compared to evapotranspiration derived with an atmospheric budget analysis. The inter-comparison analyses are based on mean quantities for the period 1980–1986. Analysis of the spatial patterns of energy fluxes is based on mean results for July, which is generally similar to other summer months. A winter month was not selected to avoid possible complications due to snow and cold weather processes.

Earlier PILPS experiments, such as Phase 2(a), were limited to comparisons of energy fluxes over an equilibrium year. In contrast, the Phase 2(c) comparisons were for multiple years, and the simulation region is a continental scale basin with a diverse climate, which allows assessment of space-time differences in energy fluxes among models.

2. Comparisons of net radiation and surface temperature

The surface net radiation is given by:

$$R_n = (1 - \alpha) R_s + \epsilon R_{ld} - \epsilon \sigma T_s^4 \quad (1)$$

where R_s and R_{ld} are the downward shortwave and longwave radiation, T_s is the effective surface tem-

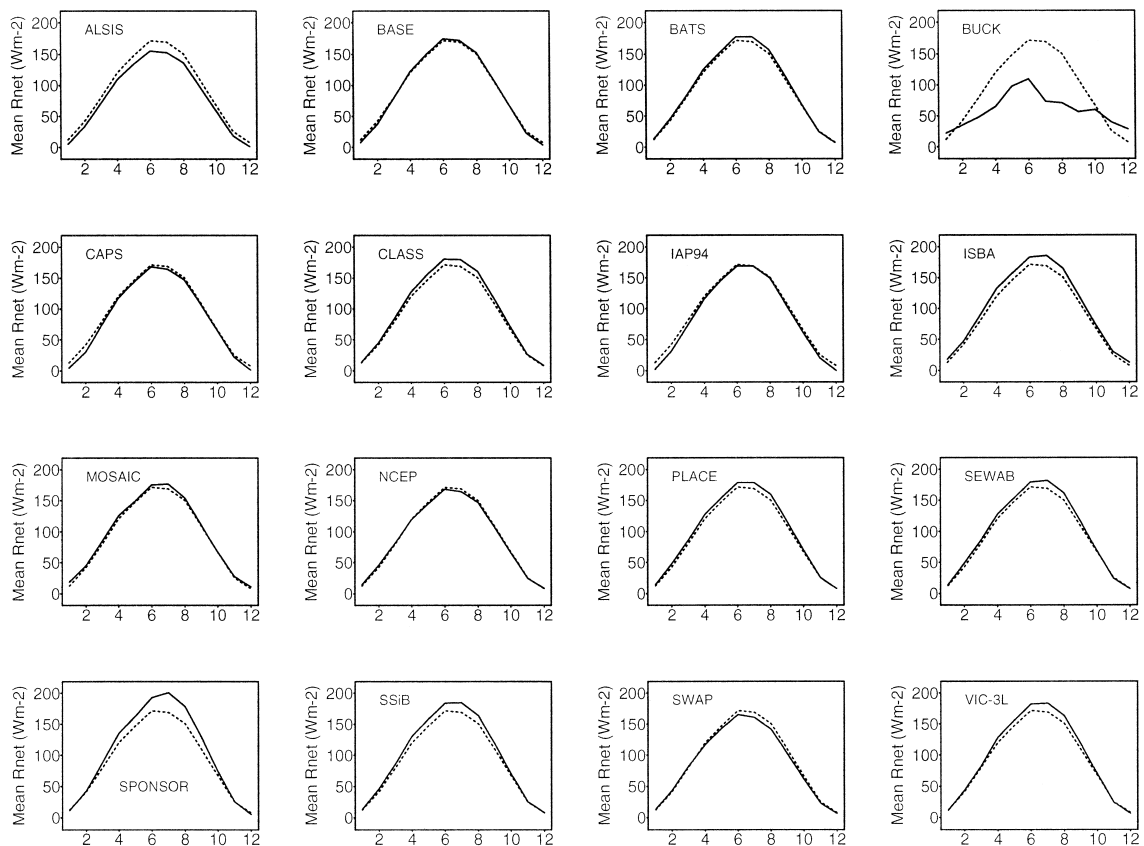


Fig. 2. Mean monthly model-simulated net radiation over the Red-Arkansas River basin (1980–1986). The dotted line is the average of the models.

perature, α is surface albedo, ϵ is the thermal emissivity (taken as 1.0 for each scheme), and σ is Stefan–Boltzmann constant. Among the variables and parameters in the right-hand side of Eq. (1), only the surface temperature and albedo vary across schemes.

The annual average net radiation for each scheme was calculated for the period 1980–1986, results of which are shown in Fig. 1a along with the mean, standard deviation, and the difference between the maximum and minimum net radiation among the 16 schemes. Also shown in Fig. 1 are the average annual net (absorbed) solar radiation, surface temperature, and latent, sensible, and ground heat fluxes. All schemes had mean annual net radiation between 80 and 105 W m^{-2} . The scheme BUCK (bucket model) was about 20 W m^{-2} lower than the others, which mostly are within 5 W m^{-2} . The main cause

for the large difference between BUCK and other schemes can be traced to its warmer mean annual surface temperature (about 5°C higher than any of the other schemes). The differences among models in the annual average absorbed solar radiation, on the other hand, are quite small. The reason for the high surface temperature in BUCK was not resolved.

Of the remaining 15 schemes, ALSIS had the smallest net radiation (81.0 W m^{-2}) and SPONSOR the highest (103.8 W m^{-2}). Of the difference in net radiation between ALSIS and SPONSOR, 63% was due to the difference in albedo (0.06) and the rest was due to the difference in surface temperature (1.76°C).

The mean seasonal cycles for net radiation, albedo, and surface temperature (solid line) are shown in Figs. 2–4 for the period 1980–1986. The seasonal patterns of net radiation are similar among models,

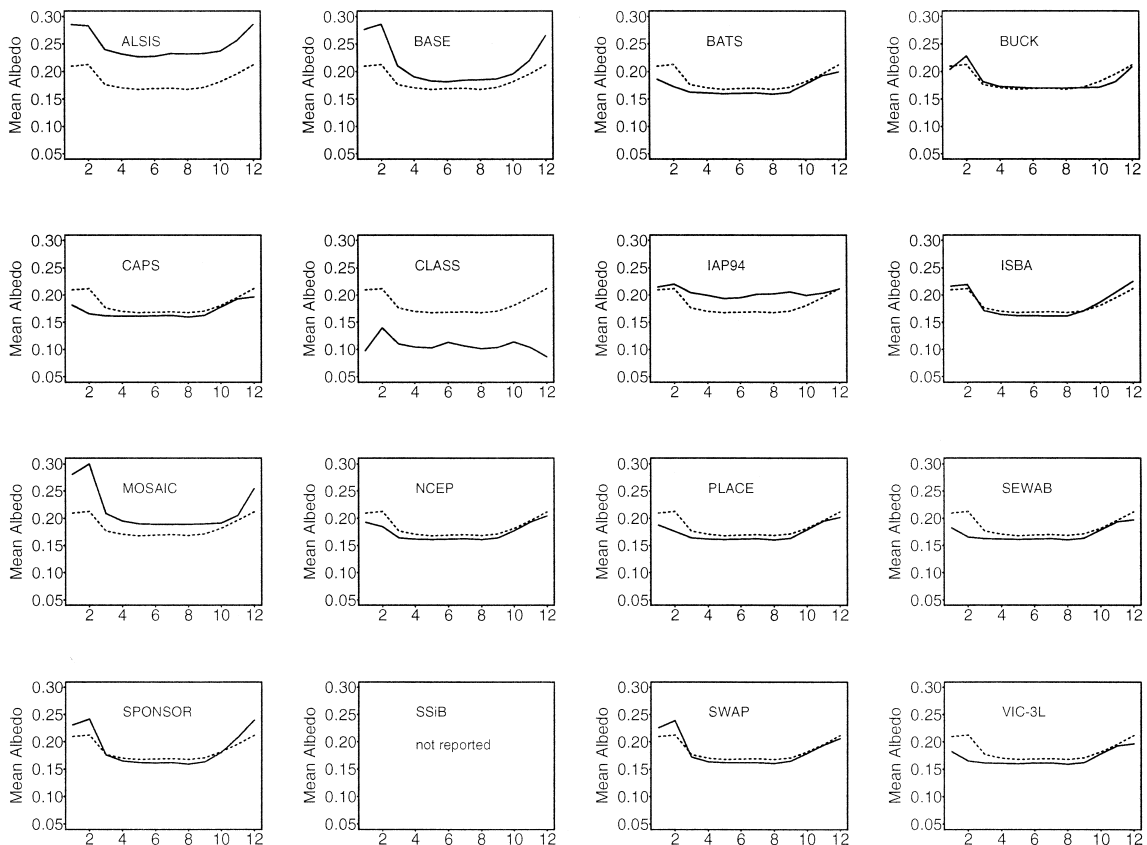


Fig. 3. Mean monthly model albedo over the Red-Arkansas River basin (1980–1986). The dotted line is the average of the models.

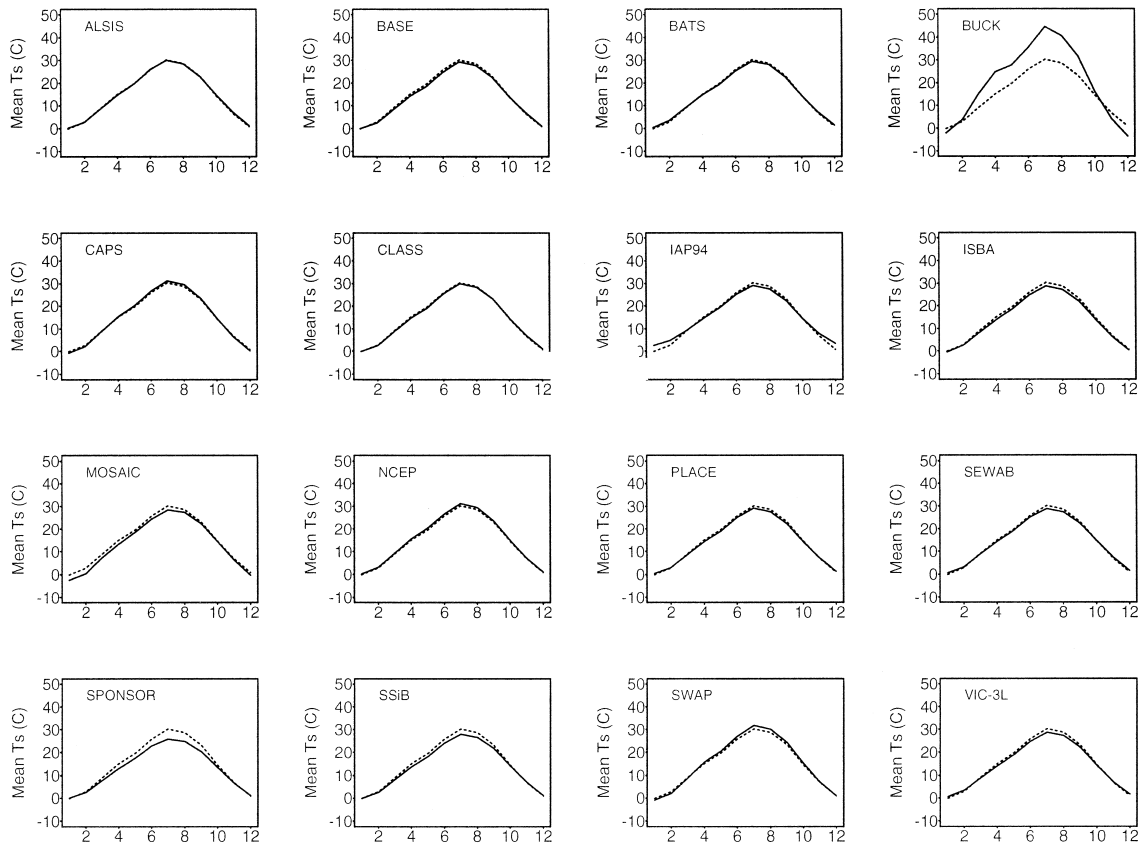


Fig. 4. Mean monthly model-simulated surface temperature over the Red-Arkansas River basin (1980–1986). The dotted line is the average of the models.

except for BUCK which had much less summer net radiation. Among the other 15 schemes, SPONSOR had the highest summer net radiation due to its lower surface temperature (Fig. 5), while ALSIS had the lowest which was caused by its higher albedo (Fig. 4). The higher net radiation of CLASS was caused mainly by its lower albedo (Fig. 4). CAPS, NCEP and SWAP had lower net radiation compared with other schemes due to their slightly higher surface temperature (Fig. 5).

BUCK had a mean monthly surface temperature of around 44°C in July (Fig. 5) which seems unrealistically high for the region. On the other hand, BUCK had the coldest December surface temperature (-3.55°C) among the 16 schemes which likewise appears to be unrealistic. The surface temperature of MOSAIC (about -2.5°C) in January was

about 2°C colder than the other models (except for BUCK). This cold January temperature may be the reason MOSAIC reported more snowmelt runoff than other schemes.

The variability in monthly net radiation (solid line) over the Red-Arkansas River basin (1980–1986), as measured by the standard deviation, is shown in Fig. 5. The dotted line in Fig. 3 is the average standard deviation of the models. BUCK had the largest variability in monthly net radiation. The range in variability is similar among the other schemes, although CAPS, MOSAIC and IAP94 had slightly higher variability in the winter. All the schemes had their largest variability in April, with the exception of BUCK (August).

The spatial distributions of the July mean model-simulated surface temperature and net radiation

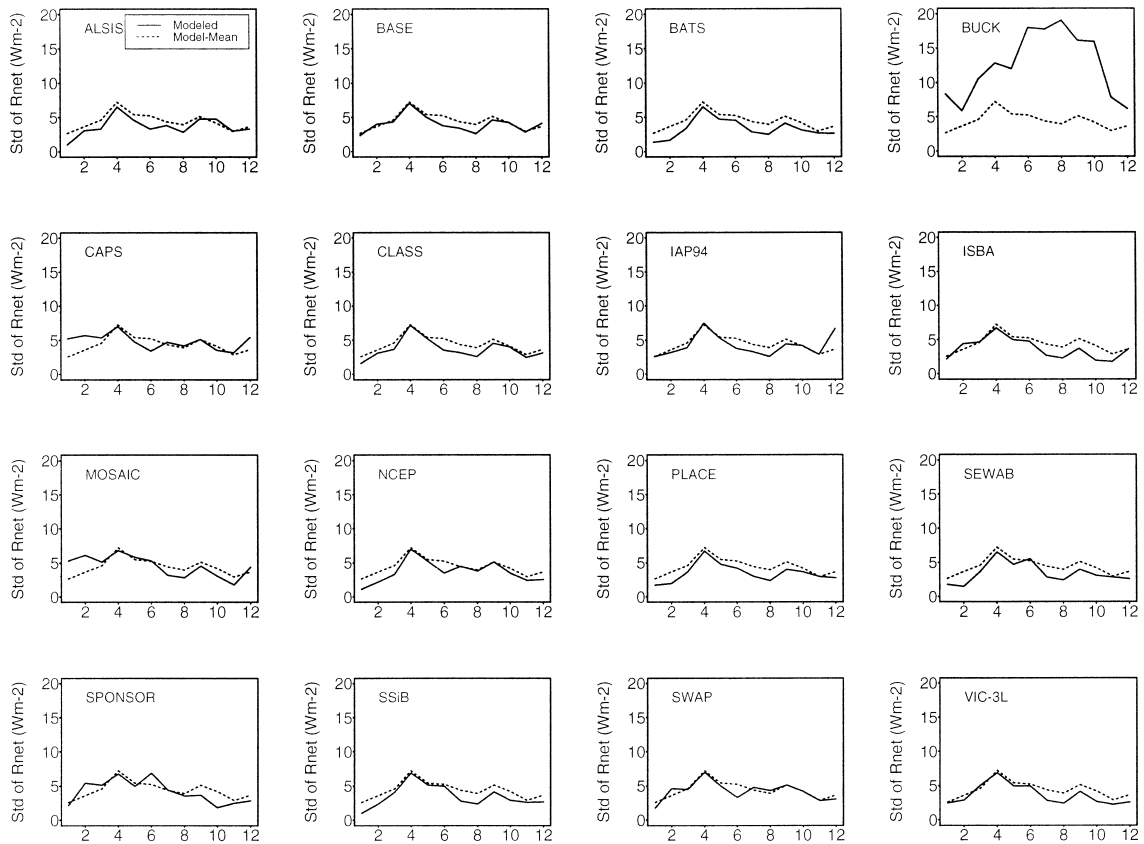


Fig. 5. Standard deviation of model-simulated monthly net radiation over the Red-Arkansas River basin (1980–1986). The dotted line is the average standard deviation of the models.

(averaged over 1980–1986) are shown in Figs. 6 and 7. The observed July mean atmospheric forcings for the same period are shown in Fig. 8. The spatial distribution for BUCK's surface temperature is quite different from those of the other models. BUCK simulated relatively low surface temperatures around the grid (34.5°N, 94.5°W), although its average surface temperature over the basin was much higher than for the other models. CAPS, NCEP and SWAP were somewhat warmer than most models, having their surface temperature maxima around 40°C. NCEP has higher surface temperatures between lat 34.5°N and 36.5°N and along long 96.5°W, which is not found in other schemes. SPONSOR had the lowest basin average surface temperature.

The spatial pattern of BUCK's simulated net radiation appears anomalous, with a mean of less than

half that of the other schemes (Figs. 2 and 7). Its low net radiation is caused by its higher surface temperature. ALSIS and SWAP had lower net radiation than the other models, while SPONSOR had higher values. ALSIS's low net radiation resulted primarily from its higher albedo (Fig. 4). SWAP's surface temperatures were higher and SPONSOR's lower than most models, resulting in lower and higher net radiation, respectively, for the two models. Most schemes (except for ALSIS, BUCK, IAP94 and NCEP) had two regions of high net radiation centered around (33.5°N, 94.5°W) and (36°N, 96.5°N). The high net radiation values in these two regions are primarily attributable to the low albedo values (Fig. 8j).

Insight into the nature of the spatial differences in net radiation among the models can be obtained by

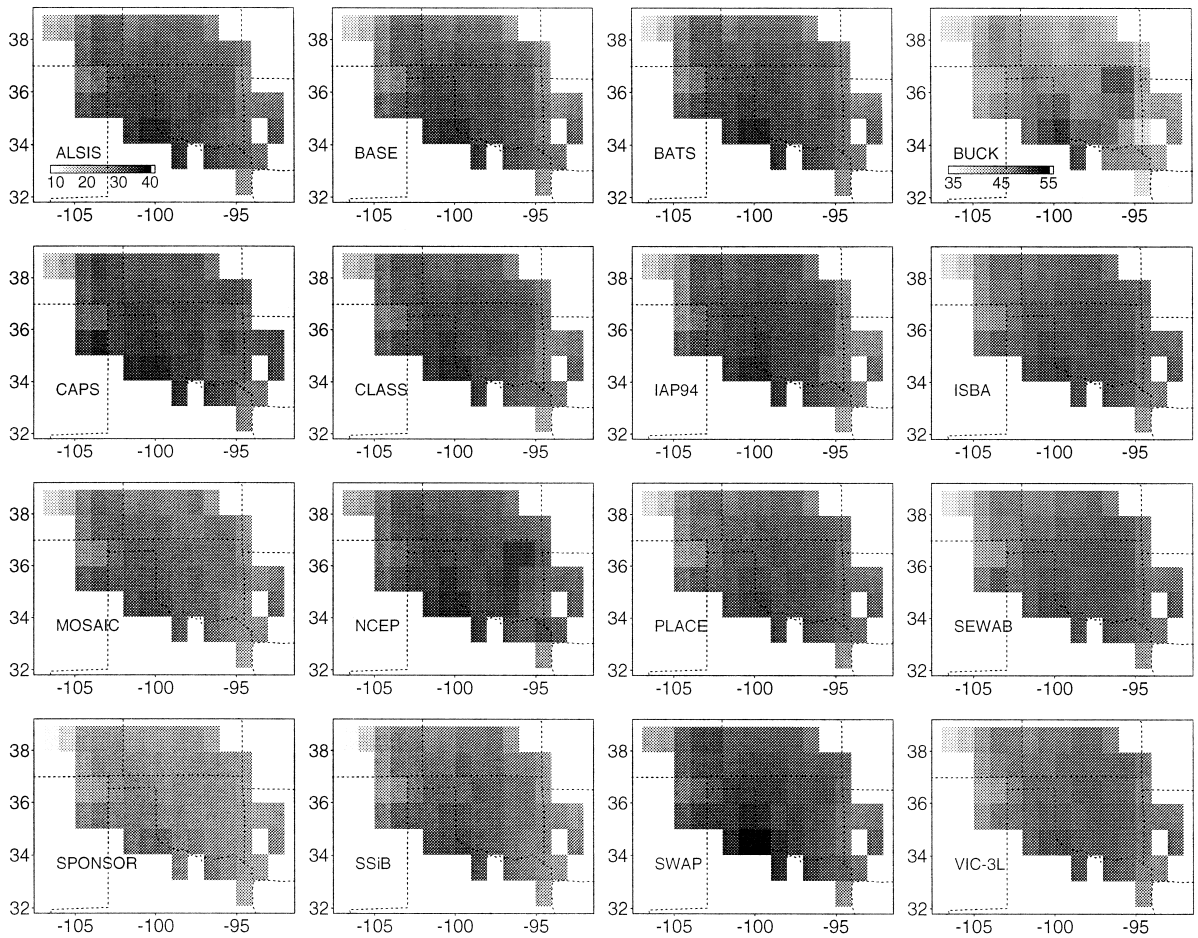


Fig. 6. Spatial distribution of model-simulated July mean (1980–1986) surface temperature (°C).

using air temperature, rather than model-computed surface temperature, in the net radiation computation. Specifically:

$$T_s = T_a(1 + \delta) \quad (2)$$

where:

$$\delta = \frac{T_s - T_a}{T_a} \quad (3)$$

Usually δ is less than 0.05, resulting in $(1 + \delta)^4$ less than 1.2. This suggests that using T_a to estimate net radiation:

$$\tilde{R}_n = (1 - \alpha)R_s + \epsilon R_{ld} - \epsilon\sigma T_a^4 \quad (4)$$

will lead to an error in the emitted longwave radiation of less than 20%, and facilitates use of air

temperature data to evaluate spatial patterns in model-simulated net radiation. The spatial pattern of the albedo used in Eq. (4) is shown in Fig. 8j. The spatial pattern of the resulting \tilde{R}_n values is shown in Fig. 8i. Fig. 8i, taken together with Fig. 8j, suggests that the two high net radiation ‘islands’ are attributable for the most part to spatial variations in albedos. However, as shown in Fig. 4, some models have albedos that differ, due to internal model formulations, from the prescribed albedo pattern shown in 8j. Comparison of spatial patterns in albedo (not shown) and in surface temperature among the models showed that the deviations especially of ALSIS and IAP94 from Fig. 8i were attributable primarily to albedo and differences of BUCK primarily to surface temperature. In NCEP, the higher surface tempera-

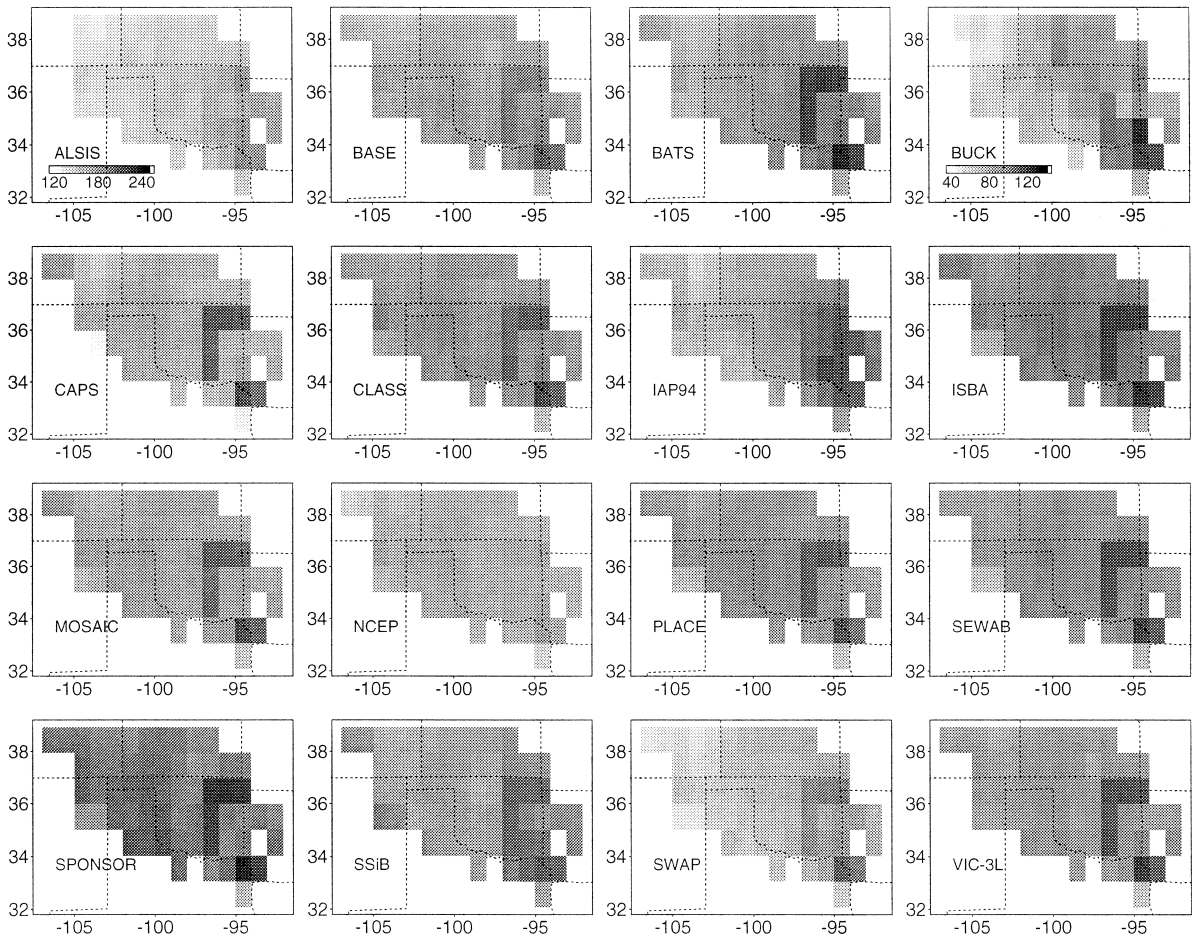


Fig. 7. Spatial distribution of model-simulated July mean (1980–1986) net radiation (W m^{-2}).

ture more or less compensated for its lower albedo values.

3. Comparison of energy heat fluxes

3.1. Latent heat flux

One of the most important functions of a land surface model is to partition the net radiation into latent, sensible, and ground heat fluxes. The maximum difference of the annual average latent heat flux among the 16 schemes was about three times smaller than that of the sensible heat flux (see Fig.

1d and e). Also, the inter-model standard deviation for the latent heat flux was about 2.5 times smaller than that for the sensible heat flux. Without BUCK, the standard deviation for the sensible heat flux was still close to two times larger than that for latent heat flux. BASE simulated the largest annual mean latent heat flux (59.53 W m^{-2}) and SPONSOR the smallest (36.20 W m^{-2}).

The mean monthly evapotranspiration for the period of 1980–1986 over the Red-Arkansas River basin is shown in Fig. 9 for each scheme. In the same figure, the mean monthly evapotranspiration over the basin estimated using an atmospheric budget analysis (Zhao, 1997) using radiosonde data for the same period is included (dotted line). The evapo-

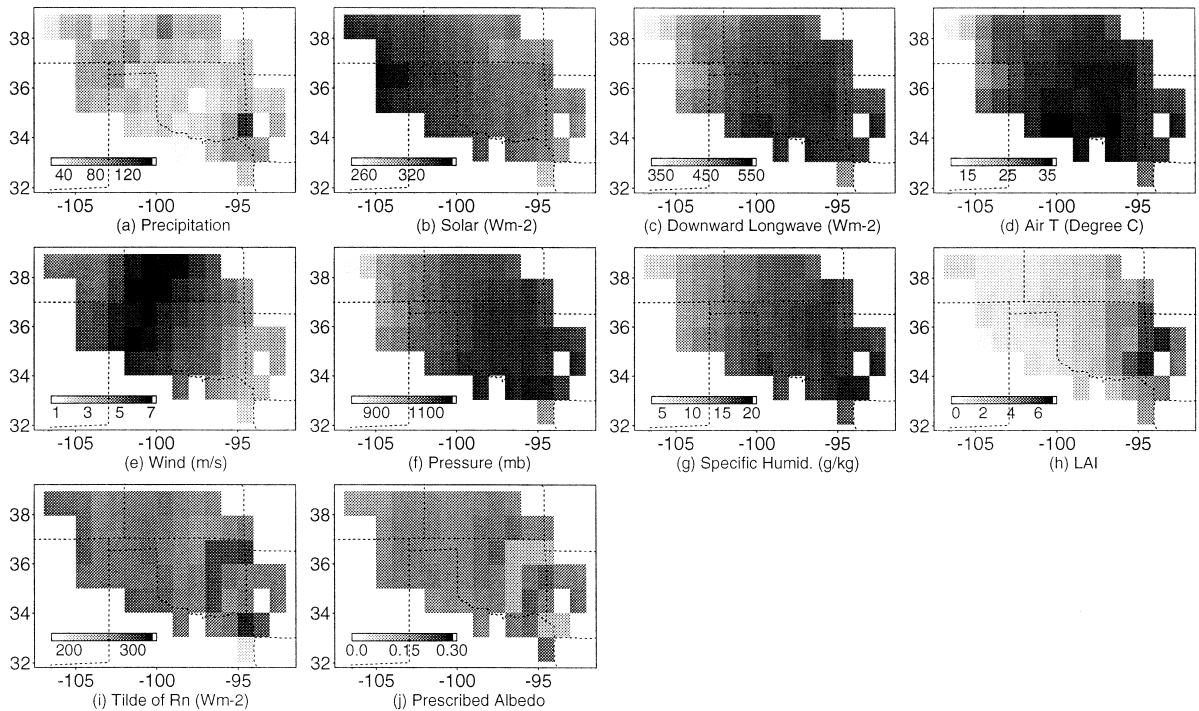


Fig. 8. Spatial distribution of observed July mean (1980–1986) atmospheric forcing, LAI, R_n (see Eq. (4)) and the prescribed albedo.

transpiration, E_{at} , from the atmospheric water vapor budget can be expressed as:

$$E_{at} = \int \frac{dq}{dt} + \nabla q \vec{v} + P \quad (5)$$

where q is the water vapor content of the atmosphere, \vec{v} is the wind speed, and P is the precipitation. Eq. (5) was evaluated twice daily and aggregated to monthly estimates of E_{at} . For the change in precipitable water (first term on the right hand side of Eq. (5)), the error is estimated to be within 10% on a monthly time step. For the convergence (second term), the monthly error is expected to be within 25% (Zhao, 1997, personal communication). This suggests that the overall estimated error for E_{at} will be within 30% on a monthly basis. However, the mean annual Red-Arkansas basin evapotranspiration estimated using Eq. (5) matches to within a few percent the evapotranspiration estimated as the difference between long-term precipitation and the sum of Arkansas and Red River outlet streamflow

(Abdulla, 1995). Furthermore, long-term basin-average precipitation and runoff are both well estimated (to within a few percent), which suggests that the error in basin-average annual evapotranspiration based on Eq. (5) is well within 5%. On a monthly basis, the errors in the Eq. (5) estimates are expected to be slightly larger, but for the peak (summer) evapotranspiration months, they should be within 10%, given that their sum is constrained to match the annual value. Therefore, for purposes of evaluating the mean monthly evapotranspiration simulated from the land surface schemes, the error in Eq. (5) is taken to be less than about 10%, except, perhaps, for the winter months, where mean values are low.

Fig. 9 shows that SPONSOR, SEWAB, ALSIS, PLACE and SWAP underestimated the mean monthly atmospheric budget evapotranspiration (expressed as latent heat flux). The underestimation in evapotranspiration in these schemes is connected to an overestimation of runoff (see Wood et al., this issue and Lohmann et al., this issue, for details). BASE consistently overestimated evapotranspiration. The rest of

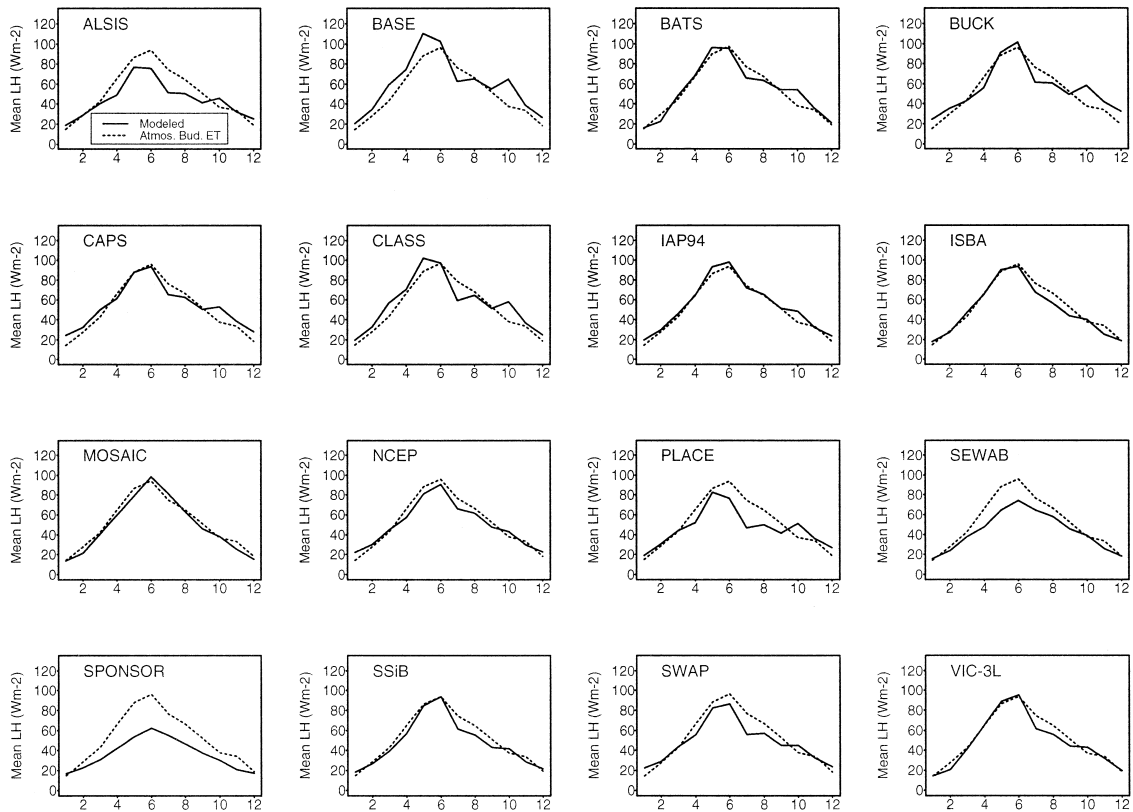


Fig. 9. Mean monthly model-simulated total latent heat flux over the Red-Arkansas River basin (1980–1986).

the models reproduced the atmospheric budget evapotranspiration quite closely.

The underestimation of the basin runoff by BASE, BUCK, CAPS, CLASS and IAP94 resulted in only small overestimation in their evapotranspiration (see Figs. 9 and 10). The reason is that the mean runoff ratio (fraction of total runoff to precipitation) in the Red-Arkansas River basin for the period 1980–1986 is about 14.8% (Lohmann et al., this issue). Therefore, large relative differences in runoff simulation have only a small effect on the model-simulated evapotranspiration.

Fig. 10 compares mean annual model-simulated evapotranspiration (y-axis) to the relative bias which is represented by the average in the warm season, April–September, of the absolute difference between mean monthly simulated and atmospheric budget evapotranspiration, normalized by the mean (for each month) of the atmospheric budget evapotranspira-

tion. All averages were taken over the seven year period 1980–1986. The ratio is expressed as:

$$r = \frac{\frac{1}{N} \sum_{i=1}^N |E_{\text{mod},i} - E_{\text{at},i}|}{\frac{1}{N} \sum_{i=1}^N E_{\text{at},i}} \quad (6)$$

where $E_{\text{mod},i}$ and $E_{\text{at},i}$ are the i th month average model-estimated evapotranspiration and the atmospheric budget estimate over the period of 1980–1986, respectively. N is the number of months (from April–September, i.e., $N = 6$). The mean annual basin evapotranspiration derived from the atmospheric budget method is shown as the dotted line in Fig. 10. The vertical dashed line represents the estimated 10% error bound for the mean evapotranspiration in the warm season. The relative (monthly)

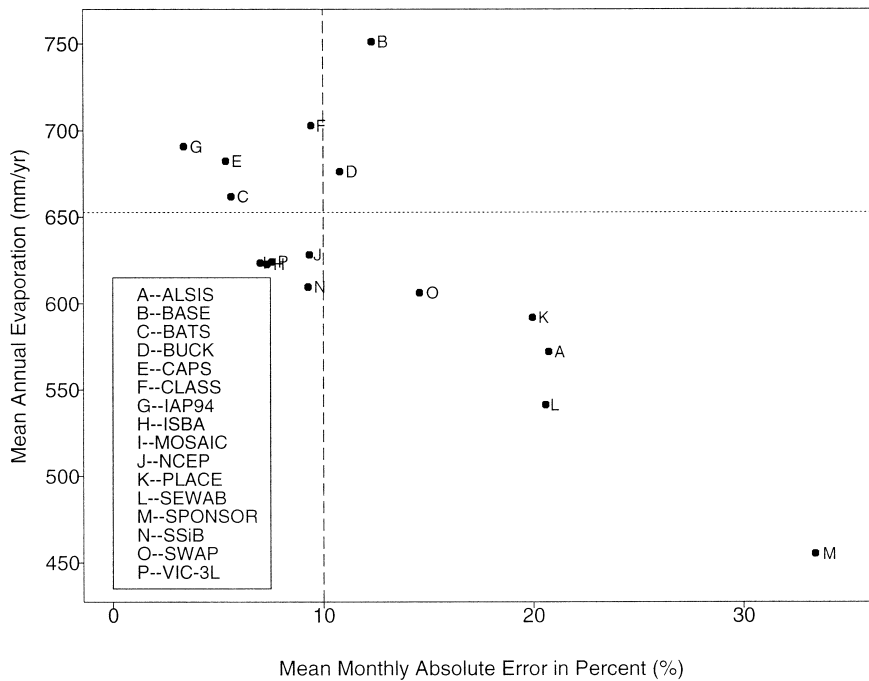


Fig. 10. Mean annual evapotranspiration versus the mean relative error for the warm season months. The relative error is the absolute difference between mean monthly simulated and atmospheric budget evapotranspiration normalized by the mean monthly atmospheric budget evapotranspiration.

biases in basin-wide evapotranspiration range from a few percent (IAP94) to more than 30% (SPONSOR), with most schemes having monthly biases of 10% or less (Fig. 10), which, as noted above, is the estimated error for the atmospheric budget estimates. ALSIS, PLACE, SEWAB, SPONSOR and SWAP have larger monthly errors than the estimated atmospheric budget error. Ten schemes reproduce the atmospheric budget annual mean evapotranspiration to within its estimated error of about 5%. ALSIS, BASE, PLACE, SEWAB and SPONSOR have larger errors. It should be noted that even schemes with relatively small errors in evapotranspiration can be associated with much larger relative errors in runoff due to the low overall runoff ratio (14.8%) for the Red-Arkansas basin.

The reasons that some schemes perform better than others with respect to their simulated evapotranspiration are complicated. Further analysis of the total evapotranspiration, its partitioning into canopy evaporation, transpiration, and bare soil evaporation, its relationship with soil moisture, and the roles of

surface and aerodynamic resistances may provide insight into differences among the schemes.

Fig. 11 shows standard deviations of the monthly latent heat flux of each scheme (solid line) and of the atmospheric budget estimate (dotted line) for 1980–1986. It is seen that most schemes have less variability than the atmospheric budget estimates. This would be expected, because the atmospheric budget estimates incorporate (relatively large) errors in the water vapor divergence term, which tend to amplify the variability of the time series of evapotranspiration estimates, especially in winter. BASE, BUCK and CLASS were more variable than the atmospheric budget estimates from April to September, which seems unrealistic.

The spatial distribution of the mean July latent heat flux is shown in Fig. 12. All of the schemes had spatial distributions similar to the spatial pattern of the July mean precipitation (Fig. 8a) that is, higher evapotranspiration areas correspond to larger precipitation totals. All of the 16 schemes had their highest evapotranspiration around the grid-box centered at

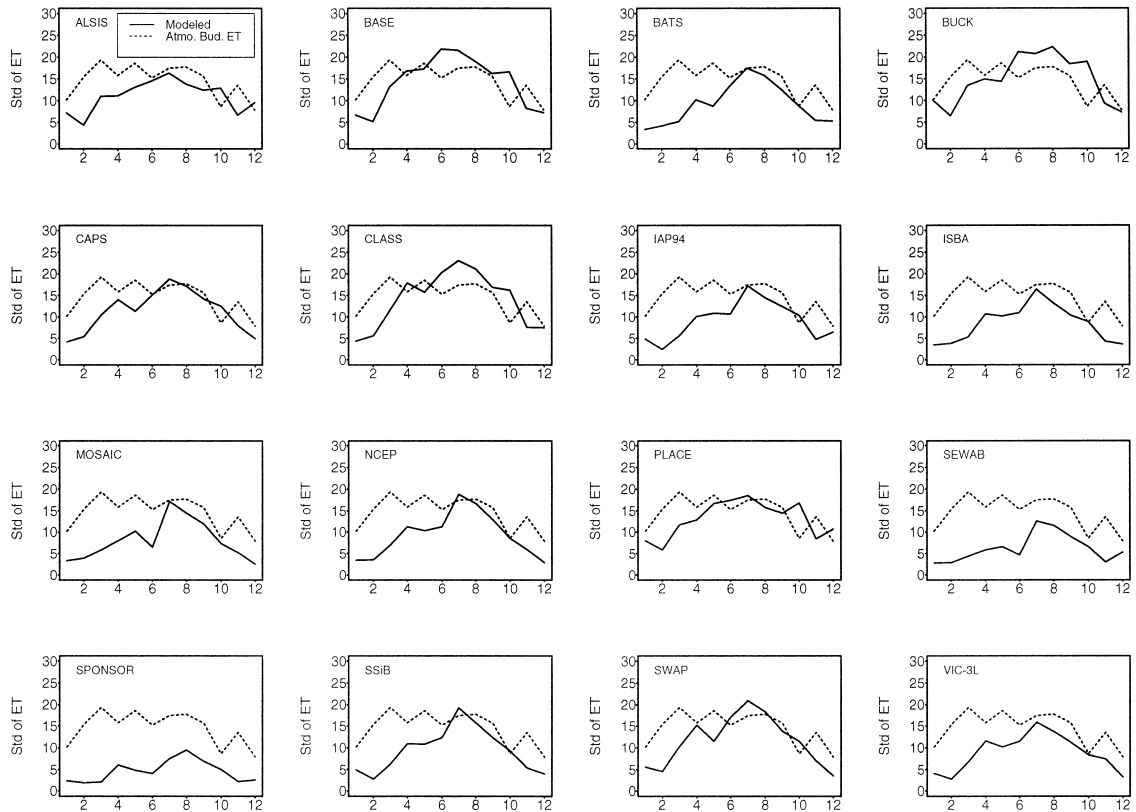


Fig. 11. Standard deviation of model-simulated basin average evapotranspiration by month (mm/month).

(34.5°N, 94.5°W) which corresponds to the area with the largest precipitation within the basin (see Figs. 8a and 12). IAP94 had relatively higher evapotranspiration values for this grid than other schemes. Over the entire basin, MOSAIC had relatively higher evapotranspiration and PLACE had relatively lower evapotranspiration than other schemes. The large surface runoff in PLACE leaves less water for infiltration, therefore less evapotranspiration from vegetation and soil.

The results suggest that the similarity in spatial patterns between the latent heat flux and precipitation occurred because during July the latent heat flux is moisture-limited rather than energy-limited over most of the basin. This is also seen from Figs. 2 and 9 in which there is a dip in latent heat for July (Fig. 9) which does not occur in the seasonal net radiation cycle (Fig. 2). Again, this suggests water limited conditions. BUCK, which had a quite different seasonal distribution for net radiation, had a seasonal

cycle for latent heat and a July spatial distribution that was similar to other schemes.

3.2. Sensible heat flux

The annual average sensible heat flux for 1980–1986 is shown in Fig. 1e. The differences among the 16 schemes were much larger than those in latent heat flux (Fig. 1d). BUCK had very small sensible heat flux (Fig. 1e), which is similar to its performance in other PILPS experiments (e.g., Chen et al., 1997), although it had high surface temperature (Fig. 1c), which seems to be inconsistent. The mean monthly sensible heat flux for 1980–1986 is shown in Fig. 13. As in Figs. 2, 4 and 5, the dotted line in each plot represents the 16 model average monthly mean sensible heat flux, and the solid line represents each model's simulated sensible heat flux. It is seen again that BUCK had very low sensible heat flux, and did not have an obvious seasonal cycle. IAP94

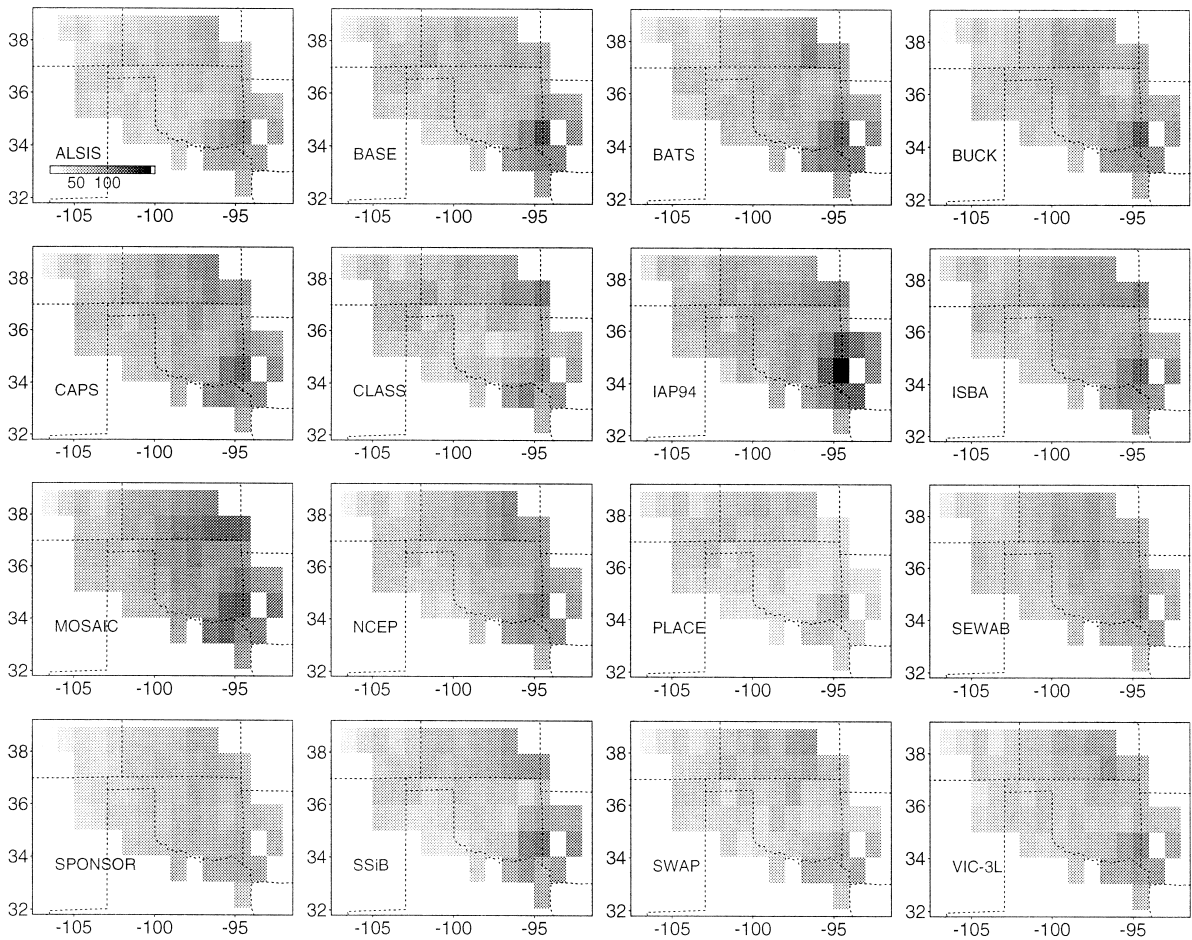


Fig. 12. Spatial distribution of model-simulated July mean (1980–1986) latent heat flux (W m^{-2}).

had low sensible heat flux due to its partitioning between sensible and ground heat flux (see Fig. 1a and f), and its seasonal cycle displays unusually high sensible heat flux in the winter time. SPONSOR had the highest sensible heat flux in most of the months due to the combination of its high net radiation and lower latent heat flux (see Figs. 2 and 9).

Fig. 14 shows the standard deviations of monthly sensible heat flux of each scheme (solid line) and of the model average (dotted line) over the Red-Arkansas River basin for 1980–1986. BASE and CLASS show the largest variability for most months of the year, while BUCK had the smallest variability among the schemes. The variability of IAP94 in the winter time was quite high. From Figs. 9, 11, 13 and

14, it is seen that some schemes that had similar mean monthly latent and/or sensible heat fluxes had quite different interannual variability. This emphasizes the importance of analysing multiple annual cycles and not just one specific year.

The spatial distribution of the July mean sensible heat flux is shown in Fig. 15. All but two of the schemes had high sensible heat flux regions centered around (33.5°N , 94.5°W) and (36.5°N , 96.5°W). The locations and shapes of these two regions (i.e., the ‘islands’) were similar to the regions of high net radiation (see Fig. 7). The results from ALSIS, BUCK, IAP94 and NCEP did not show these regions in their net radiation (see Fig. 7) and IAP94 and NCEP did not have the two regions of high sensible

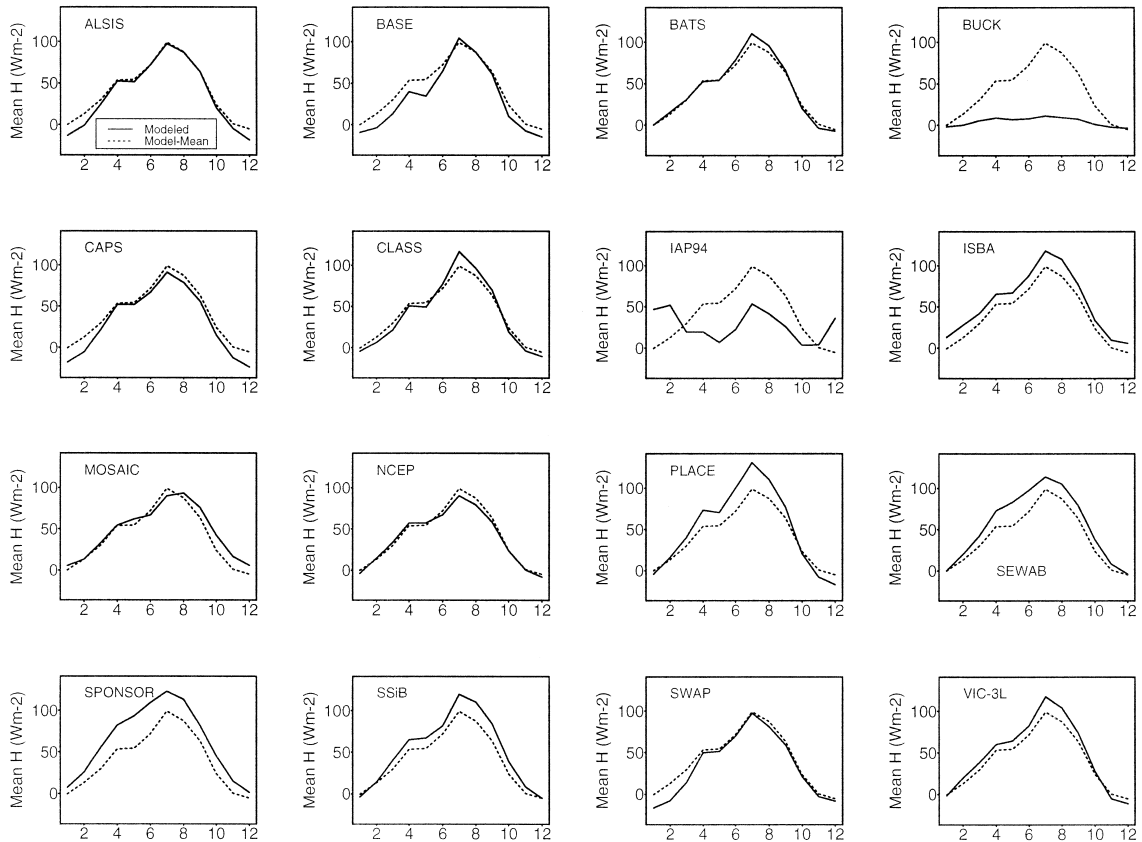


Fig. 13. Mean monthly model-simulated sensible heat flux over the Red-Arkansas River basin (1980–1986). The dotted line is the average of the models.

heat flux (Fig. 15). The reason for NCEP is that it has the highest values of its aerodynamic resistance for sensible heat flux in this regions, opposed to other models.

The relatively high sensible heat flux along the southwest basin boundary corresponds to the high surface temperature in that area. BUCK had by far the lowest sensible heat flux across the basin. CAPS, IAP94, MOSAIC and NCEP had lower sensible heat flux than the other schemes in general, while PLACE had higher values. The differences of magnitudes and patterns in the temporal seasonal cycles (Fig. 13) among the schemes (excluding BUCK and IAP94) were generally smaller than those for the spatial distributions (Fig. 15). Also, the differences in magnitudes in the spatial distribution of the sensible heat flux were larger than in the spatial distribution of the latent heat flux (Fig. 12). This is possibly due to the

fact that the evaporative process is constrained by the water budget.

3.3. Ground heat flux

Fig. 1f shows that among the energy components the annual average ground heat flux had the largest variability relative to its mean. The mean monthly ground heat flux for 1980–1986 is shown in Fig. 16. The monthly measured ground heat fluxes from CABAUW (the Netherlands), HAPEX (France) and ABRACOS (Brazil) are also plotted in Fig. 16 with symbols C, H and A, respectively. Although the climatology over the Red-Arkansas basin is quite different from these sites, the data are nonetheless useful as a point of reference. BUCK does not estimate the ground heat flux and is not included in the following analysis.

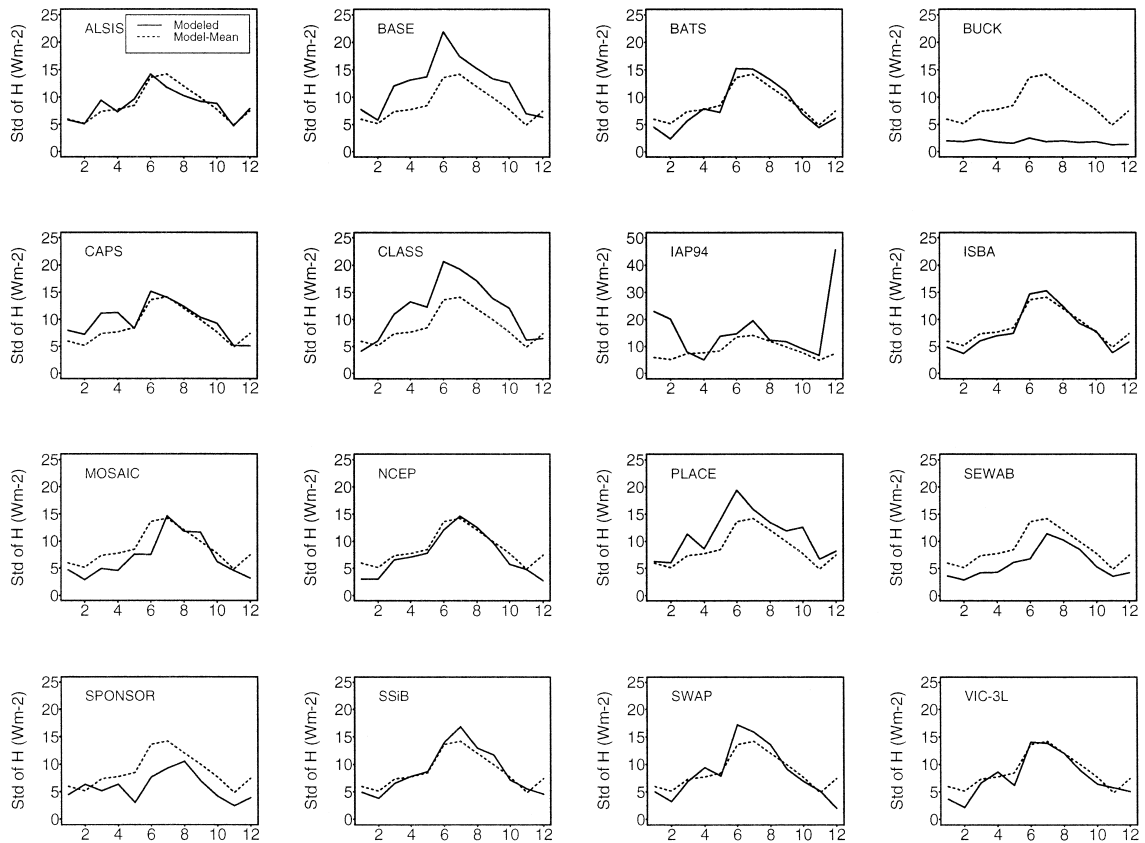


Fig. 14. Standard deviation of model-simulated monthly sensible heat flux over the Red-Arkansas River basin (1980–1986). The dotted line is the average standard deviation of the models.

Fig. 16 shows that IAP94, SPONSOR and SWAP had a seasonal range that differed significantly from the other schemes. IAP94 simulates ground heat flux as a residual of the energy balance equation. Its unusual seasonal cycle and the small magnitudes of its sensible heat flux probably affected its ground heat flux. IAP94, SPONSOR and SWAP all appear to have an annual range that was too large by comparison to the other models and with data from the three sites mentioned above.

The seasonal cycles of the schemes can be divided into three groups. One group, CAPS, IAP94, ISBA, NCEP and SPONSOR, had a 'bell' shape that is similar to their seasonal cycles of net radiation (see Fig. 2). The remaining schemes (except for SWAP) had shapes closer to a sine function with the ground heat flux reaching its annual maximum earlier than net radiation. SWAP is an exception whose

ground heat flux cycle differed in shape from any of the other schemes.

Fig. 17 shows the spatial distribution of mean July ground heat flux for 1980–1986. There was much less agreement with respect to the patterns and magnitudes for the ground heat flux among the schemes than for the other energy components. ISBA and PLACE had the lowest values among the schemes, less than 2 W m^{-2} over the region. In contrast, IAP94 had ground heat flux values higher than 20 W m^{-2} over most of the region, with more than 100 W m^{-2} in the vicinity of $(35.5^\circ\text{N}, 94.5^\circ\text{W})$. For the remaining schemes, their ground heat fluxes varied between 0 and 30 W m^{-2} (see Fig. 17).

As in the cases of latent and sensible heat fluxes, there were no observations of the magnitudes and spatial distribution of ground heat flux for the Red-Arkansas region. However, a general spatial pattern

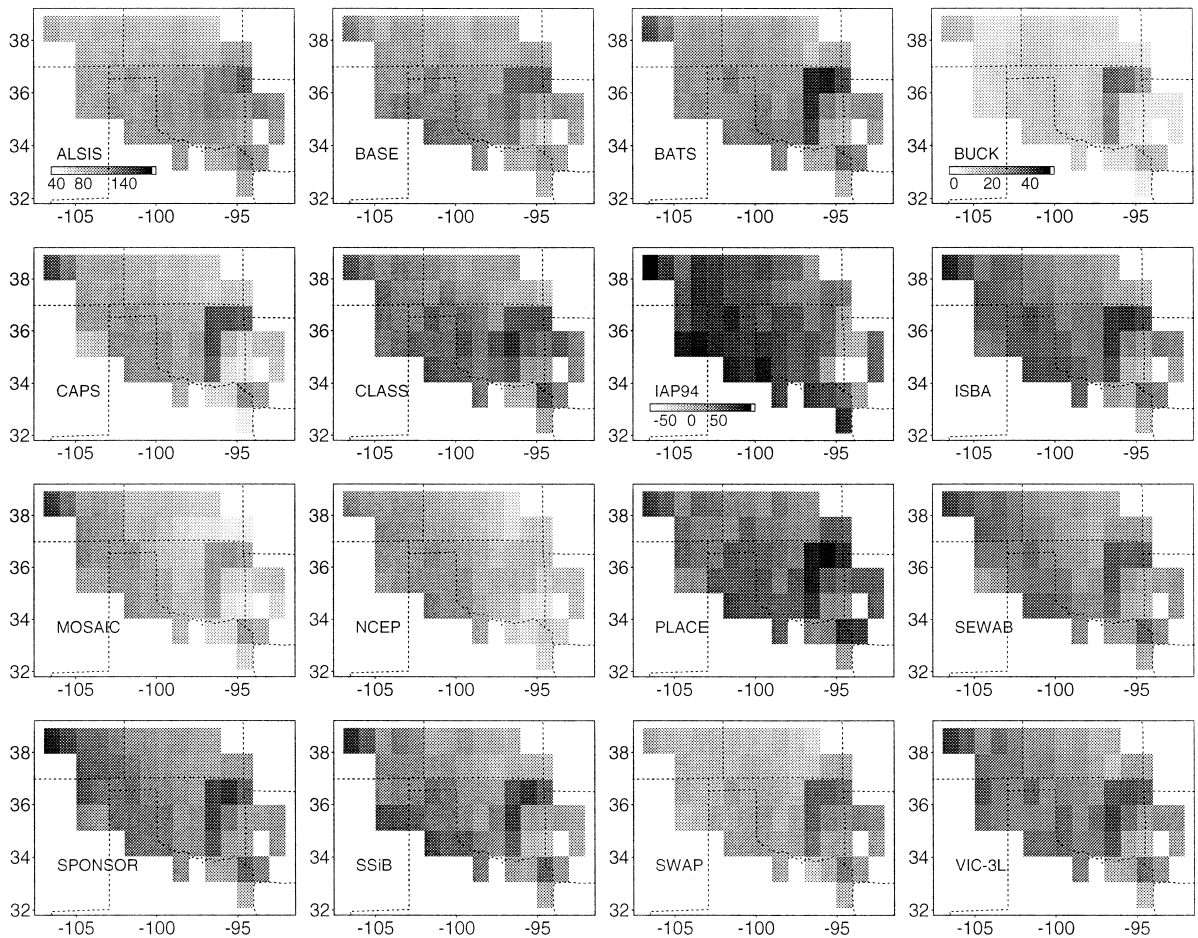


Fig. 15. Spatial distribution of model-simulated July mean (1980–1986) sensible heat flux (W m^{-2}).

of the ground heat flux can be inferred from field measurements that show that under similar net radiation conditions the ground heat flux is lower under a full vegetation canopy than under sparse vegetation and for bare soil surfaces (e.g., Clothier et al., 1986; Choudhury et al., 1987; Kustas and Daughtry, 1990). Fig. 8h shows the July mean spatial distribution of leaf area index (LAI), from which it can be seen that the eastern portion of the basin has much higher LAIs than the middle and western portion. From the earlier net radiation discussion (e.g., Figs. 7 and 8i), it is observed that the July mean net radiation over Red-Arkansas is rather smooth (except for the two high value 'islands'). Therefore, it can be seen that the July mean spatial distribution of ground heat flux should have lower magnitudes in the eastern portion

than in the western and the middle portions of the basin.

ALISIS, BASE, BATS, CLASS, PLACE, SEWAB, SPONSOR and VIC-3L all show lower ground heat fluxes in the eastern portion and higher values in the western and middle portion of the basin. Some schemes have a less distinct gradient than shown in Fig. 8h for the LAI distribution, and some schemes show more spatial variability. CAPS, IAP94, ISBA, MOSAIC, NCEP and SSiB have higher ground heat flux values in the east, and lower values in the west, which is counter to the above argument. For CAPS, the apparent explanation is that the thermal diffusion equation is applied to vegetated areas under an implicit assumption of bare soil conditions. This formulation will be revised in a subsequent version of

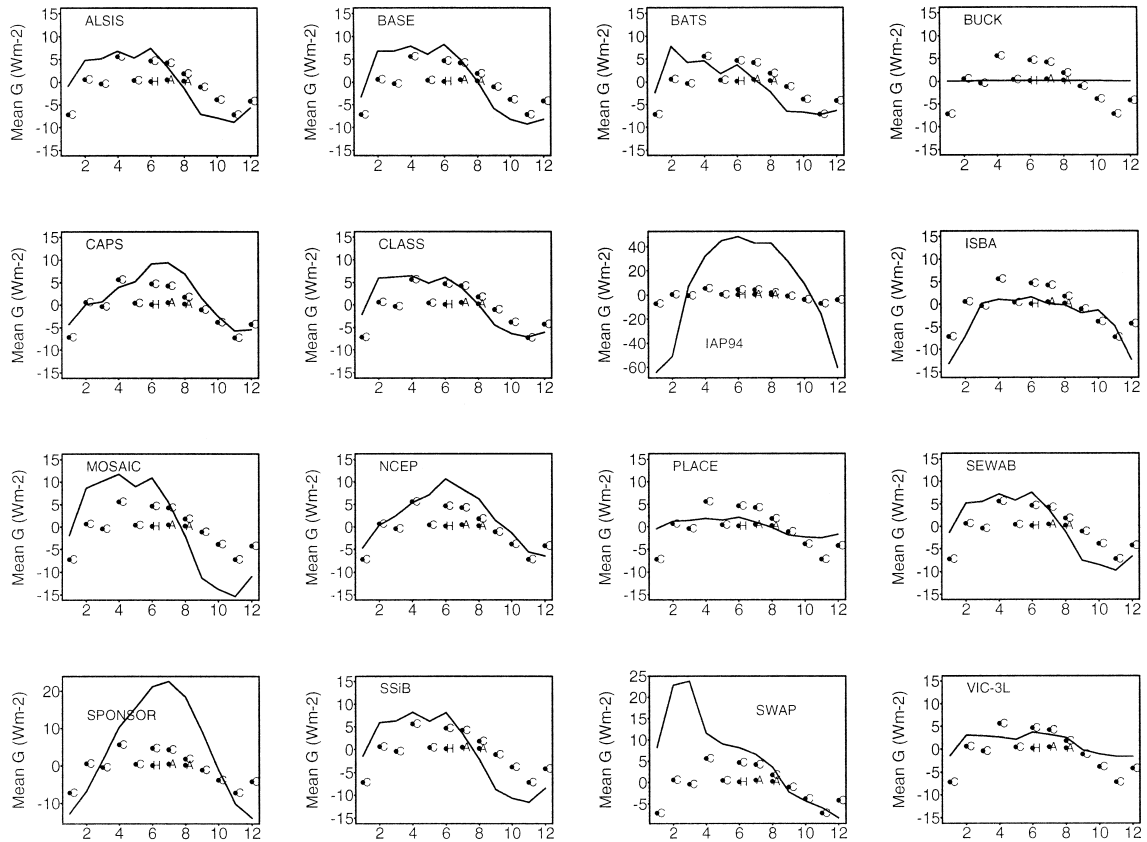


Fig. 16. Mean monthly model-simulated ground heat flux over the Red-Arkansas River basin (1980–1986). The symbols of C, H, and A represent the monthly measured ground heat fluxes from CABAuw (the Netherlands), HAPEX (France), and ABRACOS (Brazil), respectively. BUCK does not estimate the ground heat flux and is set to zero in this plot.

CAPS. The spatial distribution for NCEP seems questionable, as its ground heat flux is the highest in the region where the LAI is the largest, and the lowest in the region where it has the smallest LAI. The spatial pattern of SWAP is also unusual.

To further examine the effects of vegetation on ground heat flux, two grid cells with different LAIs were selected. The July mean LAI at grid cell A (35.5°N, 94.5°W) is 5.3 (cultivated crops), and at B (33.5°N, 96.5°W) it is 1.3 (grassland). The July mean diurnal net radiation cycles for the two grid cells for each of the models are shown in Fig. 18. Generally, the difference in net radiation at A and B was quite small among the 15 schemes that reported the necessary information. Some schemes were less smooth than others, due to differences in the model time

steps (see Table 1 of Wood et al., this issue). Fig. 19 shows the July mean diurnal ground heat flux for each scheme. An important observation from Fig. 19 is that most schemes did not have smaller ground heat flux at grid cell A when compared to B, even though the LAI at A is about 4 times larger than the LAI at B. CAPS, IAP94, NCEP, SEWAB and SWAP simulated higher ground heat flux at grid cell A than at B. BATS, MOSAIC, PLACE, SPONSOR and SSiB had almost the same ground heat flux at A and B. Schemes that had lower ground heat fluxes in the higher vegetated areas include ALSIS, BASE, CLASS, ISBA and VIC-3L. This pattern is generally consistent with Fig. 17.

An empirical equation that relates midday ground heat flux to net radiation (R_n) and LAI is expressed

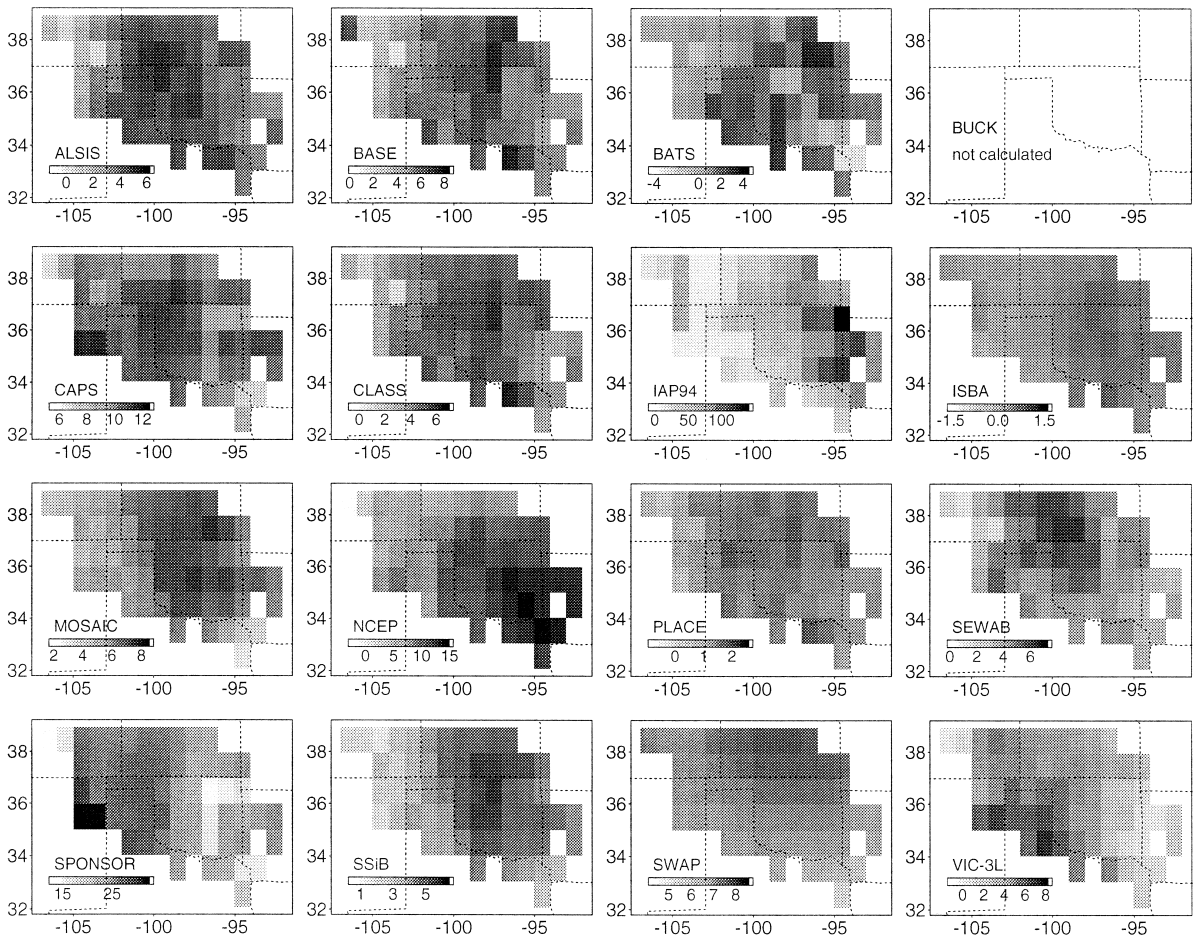


Fig. 17. Spatial distribution of model-simulated July mean (1980–1986) ground heat flux ($W m^{-2}$).

as (Fuchs and Hadas, 1972; Idso et al., 1975; Choudhury et al., 1987; Huang and Lyons, 1995):

$$G = \beta \exp(-\gamma LAI) R_n \quad (7)$$

Eq. (7) applies to the midday values of G , which generally have different phase from R_n . Based on field measurements, β varies between 0.22 and 0.51 (Idso et al., 1975), and γ varies between 0.45 and 0.65 for various crops (Mouteith, 1973). Using these values, Choudhury et al. (1987) postulated a likely range of G for a growing crop as:

$$0.2 \exp(-0.65 LAI) R_n \leq G \leq 0.5 \exp(-0.45 LAI) R_n \quad (8)$$

Using the average July mean diurnal net radiation from each scheme, the upper and lower bounds of G from Eq. (8) are shown in Fig. 20 as possible lines of reference, together with the modeled midday G at grid A. SWAP and VIC-3L had midday ground heat flux within the estimated bounds, but SWAP had essentially no diurnal variation, which seems unreasonable. The remaining 13 schemes all had midday ground heat fluxes higher than the estimated upper bound, with BATS, PLACE and SSiB slightly exceeding it. All of the schemes except for BATS and IAP94 peak earlier than net radiation. Observational studies (e.g., Fuchs and Hadas, 1972) show that, under bare soil conditions, the ground heat flux reaches its peak earlier than net radiation when soil

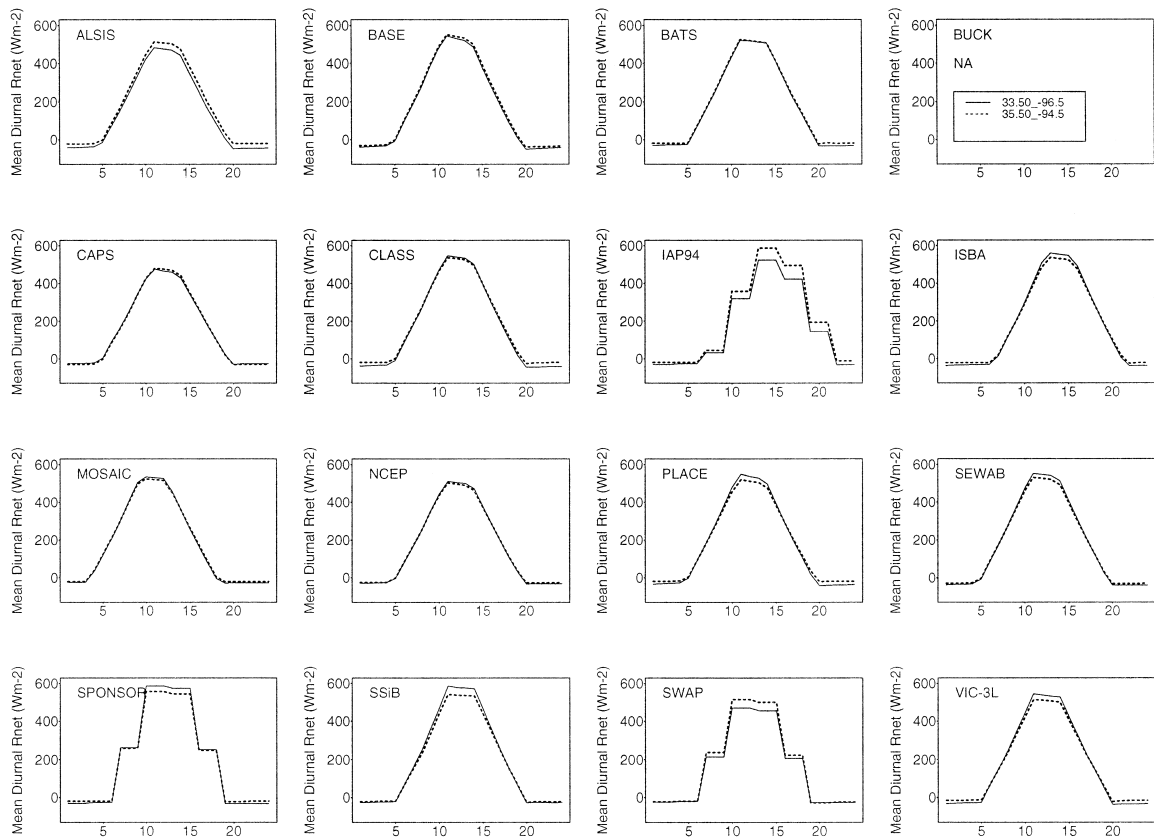


Fig. 18. July mean (1980–1986) diurnal net radiation at two grid cells.

is dry, or at about the same time when soil is wet. Huang and Lyons (1995) showed that, for some vegetated surfaces, G can lag R_n . Therefore, the exact diurnal phase differences between G and R_n depend on LAI, moisture content, and possibly many other factors. As pointed out earlier, Eq. (8) is valid only for midday hours, thus it cannot be used to evaluate the ground heat flux at other times.

Unlike grid cell A, the July mean midday diurnal ground heat flux for all schemes, except BATS, PLACE and SWAP, were within the estimated upper and lower bounds (Eq. (8)) at grid cell B (LAI = 1.3; figure not shown). As at grid cell A, BATS and IAP94 had their ground heat flux peak shifted after the peak of the net radiation, which is only possible if the peak in the sum of sensible and latent heat fluxes precedes the peak in net radiation. SWAP, as at grid cell A, had no diurnal cycle. Taken together,

the results for both test locations show that most of the schemes simulated reasonable ground heat flux at the lower LAI site. But, among the five schemes (AL SIS, BASE, CLASS, ISBA and VIC-3L) that simulated smaller ground heat flux under denser vegetation (Fig. 19), all but VIC-3L appear to underestimate the vegetation effects.

The reasons that many of the schemes had higher ground heat flux for the larger LAI regions have not been investigated. Some possibilities are: (i) failure to absorb and/or reflect the correct amount of short wave radiation by the canopy; (ii) overestimation of the soil thermal conductivity under the vegetated area (e.g., CAPS); and/or (iii) some of the schemes may not represent ground heat flux in the traditional sense, i.e., as the heat flux across the soil surface. Some schemes (e.g., MOSAIC) follow bulk soil/canopy conditions and do not attempt to isolate

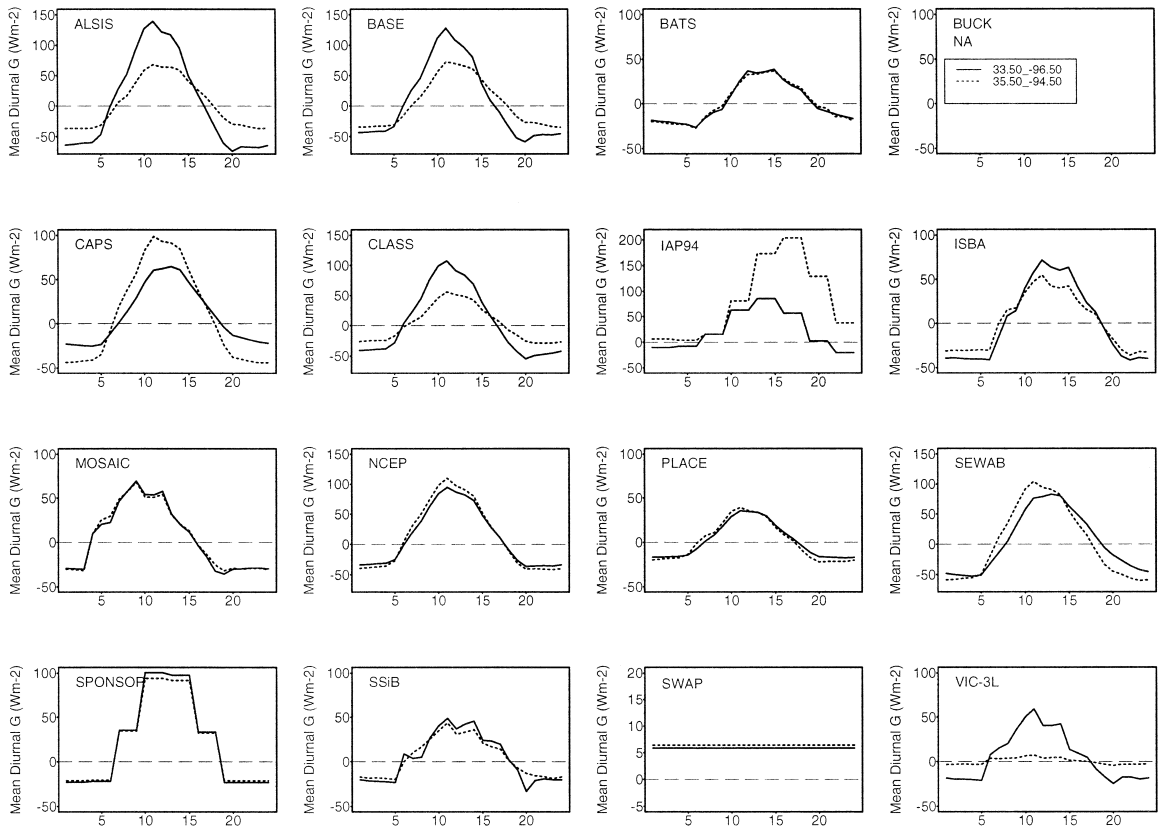


Fig. 19. July mean (1980–1986) diurnal ground heat flux at two grid cells.

this component of the bulk system heating. These differences among schemes imply that extreme caution must be exercised in comparing modeled values with measured ground heat fluxes in model calibration and validation.

4. Conclusions

Using the base-run results from PILPS Phase 2(c), intercomparisons and analyzes of the temporal and spatial distributions of the energy balance terms lead to the following conclusions.

(1) For sensible and latent heat, there was general agreement among schemes with respect to the monthly magnitudes and seasonal patterns. There was less agreement with the monthly standard deviations and with spatial distributions. For annual and

monthly mean net radiation and surface temperature, all schemes had a high level of agreement except for BUCK. Although BUCK has quite high surface temperature and very low net radiation, its total latent heat flux was comparable with most of other schemes, and with the estimated latent heat flux from the atmospheric budget method. The agreement among the schemes was closer for latent heat flux than that for sensible heat flux.

(2) Comparisons of modeled latent heat fluxes to latent heat flux estimated from an independent, radiosonde-based atmospheric budget approach showed that most (slightly more than half) of the schemes reproduced the atmospheric budget evapotranspiration (Figs. 9 and 10) to within the approximated estimation errors of 5 and 10% for the annual and monthly warm season (April–September) means.

(3) Many schemes appeared to have high ground heat flux for grids with dense vegetation. Some

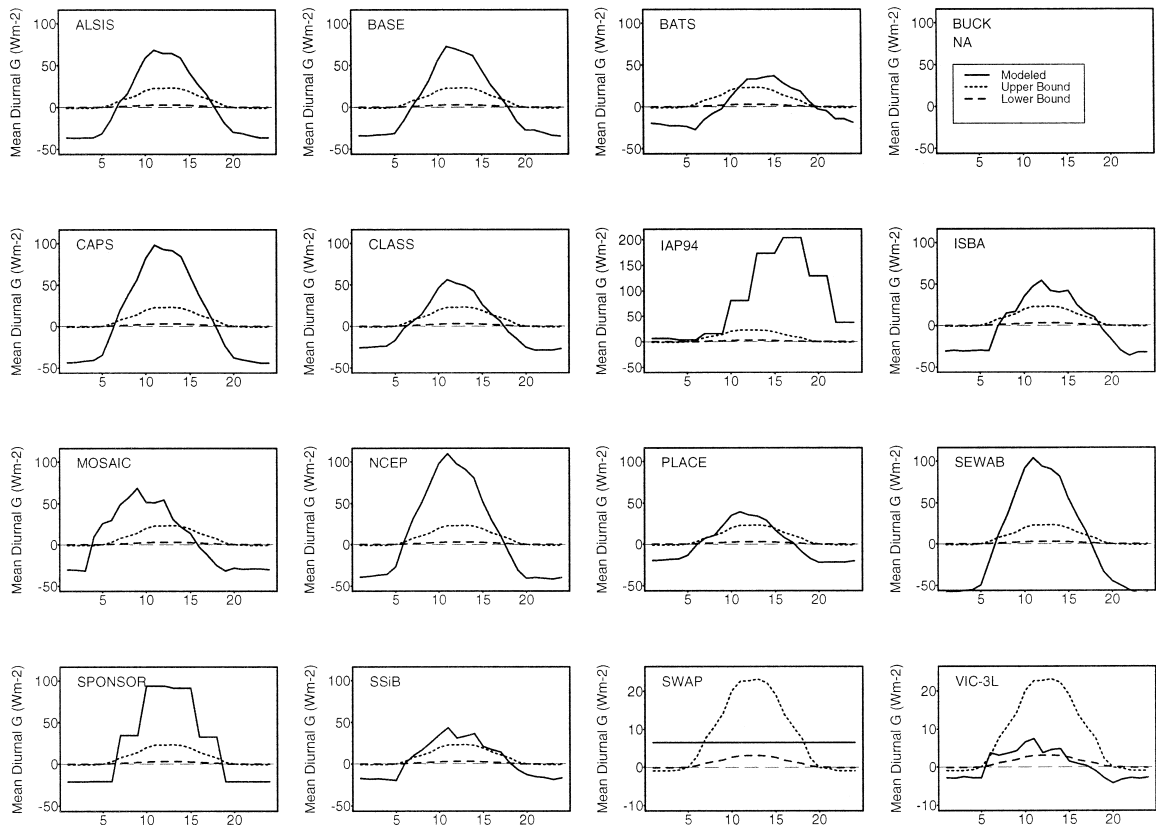


Fig. 20. July mean (1980–1986) diurnal ground heat flux at grid cell A (lat 35.5°N, long 94.5°W) with upper and lower bounds estimated from Eq. (8).

schemes have larger ground heat flux for these grids than for grids that are (relatively) unvegetated (Figs. 17, 19 and 20). This may be due to not representing properly the attenuation of short wave radiation by vegetation, overestimating the soil thermal conductivity under vegetation, and/or not interpreting within a scheme the ground heat flux as the heat flux across the soil surface.

(4) Most schemes have reasonable spatial patterns in their computed net radiation and surface temperature. The spatial patterns of latent and sensible heat flux are more variable among the schemes than the net radiation patterns. The ground heat flux spatial patterns vary greatly among the 15 schemes.

(5) Some of the schemes which have similar mean monthly latent and sensible heat fluxes have quite different monthly standard deviations of the same

quantities. This underscores the importance of carrying out model intercomparisons for multiple years, rather than focusing on one specific year.

Acknowledgements

The results presented in this paper are based on the PILPS Phase 2(c) workshop which was held from October 28–31, 1996 at Princeton University. We gratefully acknowledge Dr. Bhaskar Choudhury for his insightful inputs into the ground heat flux discussions. The PILPS Phase 2(c) activities at Princeton University were supported by NSF Grant EAR-9318896 and by the NOAA (Office of Global Programs) Grant NA56GP0249. The PILPS Phase 2(c) activities at University of Washington were

supported by NSF Grant EAR-9318898 and by NOAA/OGP Grant NA67RJ0155.

References

- Abdulla, F., 1995. Regionalization of a Macroscale Hydrological Model, PhD thesis. Department of Civil Engineering, University of Washington, USA.
- Chen, T., Henderson-Sellers, A., Milly, P., Pitman, A., Beljaars, A., Abramopoulos, F., Boone, A., Chang, S., Chen, F., Dai, Y., Desborough, C., Dickinson, R., Dümenil, L., Ek, M., Garratt, J., Gedney, N., Gusev, Y., Kim, J., Koster, R., Kowalczyk, E., Laval, K., Lean, J., Lettenmaier, D., Liang, X., Mahfouf, J., Mengelkamp, H.-T., Mitchell, K., Nasonova, O., Noilhan, J., Polcher, J., Robock, A., Rosenzweig, C., Schaake, J., Schlosser, C., Schulz, J.-P., Shao, Y., Shmakin, A., Verseghy, D., Wetzel, P., Wood, E., Xue, Y., Yang, Z.-L., Zeng, Q., 1997. Cabauw experimental results from the project for intercomparison of landsurface parameterization schemes (PILPS). *J. Climate* 10, 1194–1215.
- Choudhury, B., Idso, S., Reginato, R., 1987. Analysis of an empirical model for soil heat flux under a growing wheat crop for estimating evaporation by an infrared-temperature based energy balance equation. *Agric. For. Meteor.* 39, 283–297.
- Clothier, B., Clawson, K., Pinter, P., Moran, M., Reginato, R., Jackson, R., 1986. Estimation of soil heat flux from net radiation during growth of alfalfa. *Agric. For. Meteor.* 37, 319–329.
- Fuchs, M., Hadas, A., 1972. The heat flux density in a nonhomogeneous bare loessial soil. *Bound.-Layer Meteor.* 3, 191–200.
- Henderson-Sellers, A., Yang, Z.-L., Dickinson, R., 1993. The project of intercomparison of land-surface parameterization schemes. *Bull. Am. Meteor. Soc.* 74, 1335–1349.
- Henderson-Sellers, A., Pitman, A., Love, P., Irannejad, P., Chen, T., 1995. The project of intercomparison of land-surface parameterization schemes (PILPS): phases 2 and 3. *Bull. Am. Meteor. Soc.* 94, 189–503.
- Huang, X., Lyons, T., 1995. The simulation of surface heat fluxes in a land surface–atmosphere model. *J. Appl. Meteor.* 34, 1099–1111.
- Idso, S., Aase, J., Jackson, R., 1975. Net radiation–soil heat flux relations as influenced by soil water content variations. *Bound.-Layer Meteor.* 9, 113–122.
- Kustas, W., Daughtry, C., 1990. Estimation of soil heat flux/net radiation ratio from spectral data. *Agric. For. Meteor.* 19, 205–223.
- Lohmann, D., Lettenmaier, D., Liang, X., Wood, E., Boone, A., Chang, S., Chen, F., Dai, Y., Desborough, C., Dickinson, R., Duan, Q., Ek, M., Gusev, Y., Habets, F., Irannejad, P., Koster, R., Mitchell, K., Nasonova, O., Noilhan, J., Schaake, J., Schlosser, A., Shao, Y., Shmakin, A., Verseghy, D., Wang, J., Warrach, K., Wetzel, P., Xue, Y., Yang, Z., Zeng, Q., this issue. The Project for Intercomparison of Land-Surface Parameterization Schemes (PILPS) Phase 2(c) Red-Arkansas River basin Experiment: 3. Spatial and Temporal Analysis of Water Fluxes. *Global and Planetary Change*.
- Moutheith, J., 1973. *Principles of Environmental Physics*. Edward Arnold, London.
- Pitman et al., 1993.
- Shao, Y., Anne, R., Henderson-Sellers, A., Irannejad, P., Thornton, P., Liang, X., Chen, T., Ciret, C., Desborough, C., Balachova, O., Haxeltine, A., Ducharne, A., 1994. Soil moisture simulation: a report to the RICE and PILPS workshop. IGPO publication 14. GEWEX. PILPS. Climatic Impact Center.
- Wood, E., Lettenmaier, D., Liang, X., Lohmann, D., Boone, A., Chang, S., Chen, F., Dai, Y., Dickinson, R., Duan, Q., Ek, M., Gusev, Y., Habets, F., Irannejad, P., Koster, R., Mitchell, K., Nasonova, O., Noilhan, J., Schaake, J., Schlosser, A., Shao, Y., Shmakin, A., Verseghy, D., Wang, J., Warrach, K., Wetzel, P., Xue, Y., Yang, Z., Zeng, Q., this issue. The Project for Intercomparison of Land-Surface Parameterization Schemes (PILPS) Phase 2(c) Red-Arkansas River Experiment: 1. Experiment Description and Summary Intercomparisons. *Global and Planetary Change*.
- Zhao, W., 1997. *Diagnostic Studies and Numerical Modeling of Heavy Rainfall in the Central Plains*, PhD thesis. Princeton University, Department of Civil Engineering and Operations Research.